JURNAL KIMIA VALENSI
p-ISSN: 2460-6065; e-ISSN: 2548-3013
Journal homepage: https://journal.uinjkt.ac.id/index.php/valensi
Research Article

Dealumination Effect on ZSM-5 as a Bimetal Fe-Co Support for The Oxidative Desulfurization Process Catalyst

Lisa Adhani[1,2], Bambang Heru Susanto[1], Mohammad Nasikin[1*]

[1]*Department of Chemical Engineering, Faculty of Engineering, Universitas Indonesia, Depok, West Java, 16424, Indonesia*
[2]*Department of Chemical Engineering, Faculty of Engineering, Universitas Bhayangkara Jakarta Raya, Pasar Minggu, South Jakarta, 12550, Indonesia*

Email: mnasikin@che.ui.ac.id

Article Info
Received: April 16, 2024
Revised: April 17, 2024
Accepted: May 17, 2024
Online: June 08, 2024

Citation:
Adhani, L., Susanto, B. H., & Nasikin, M. (2024). Dealumination Effect on ZSM-5 as a Bimetal Fe-Co Support for The Oxidative Desulfurization Process Catalyst. *Jurnal Kimia Valensi*, *10*(1), 62 - 75.

Doi: 10.15408/jkv.v10i1.38456

Abstract

Petroleum fuel is still the main energy source today but causes environmental problems such as SOx gas emissions. The Oxidative Desulfurization (ODS) method removes sulfur from fuel under mild conditions. ZSM-5 is a catalyst framework considered promising in the ODS process but the small pores cause a steric barrier. The hydrophobic, mesoporous Fe-Co/ZSM-5Hierarchy catalyst was designed using the dealumination method with steam treatment to overcome the steric barrier and biphasic hindrances which are problems in this ODS process. The Fe-Co/ZSM-5Hierarchy catalyst is effective for the ODS process at a temperature of 45 °C, 45 min, the amount of catalyst used is 0.2 g, oxidant at an O/S ratio of 2, and without mass transfer agents. The embedded Fe-Co ratio shows effective mass activity by providing a TOF number of 205 h^{-1} on the Fe-$Co_{(5)}$/ZSM-5 Hierarchy and 157 h^{-1} on the Fe-$Co_{(15)}$/ZSM-5 Hierarchy catalyst.

Keywords: Hierarchy; ODS; biphasic; steric; mesopore

1. INTRODUCTION

The combustion of burning fuel containing sulfur will cause the formation of sulfur oxide (SOx) which is toxic, corrosive, and dangerous for the environment. The European Union issued strict environmental regulations on refinery operations to produce fuel with the lowest sulfur content[1,2].

Fuel desulfurization is increasingly necessary today, not only because of increasing concerns regarding environmental and legal requirements but also because very low sulfur fuels are a key requirement in fuel cell applications. Currently, fuel sulfur content requirements are increasingly stringent to achieve net zero emissions (NZE), including Indonesia[3,4]. Refineries around the world continue to develop new processes to reduce sulfur levels in fuel.

Nowadays, it is widely known that oxidative desulfurization (ODS) is considered a new technology to achieve ultra-low desulfurization. The biggest advantage of the ODS process is that the process runs at lower reaction temperatures and pressures compared to the hydrodesulfurization process which has been used and is considered a conventional desulfurization process[5,6].

However, the ODS process has obstacles, namely, (i) the steric barrier of the large organosulfur thiophene molecule and its derivatives, (ii) the resonant nature of organosulfur, (iii) the use of non-polar oxidants which cause biphasic hindrance in the desulfurization process of organosulfur in fuel. which is non-polar (iv) the process of separating sulfone resulting from the organosulfur ODS process in fuel which is polar (v) the use of excess oxidant from stoichiometry which disrupts the reaction balance and quality of the fuel due to the presence of other reaction products besides sulfone[5].

Zeolite or ZSM-5 has attracted significant attention for the ODS process due to its high selectivity properties and adsorption capabilities. However, the pore size of ZSM-5 is dominated by 5Å, which limits its effectiveness in addressing steric hindrance problems related to large organosulfur molecules. Studies on the exploration aspect of zeolite pore engineering techniques

continue to be carried out to enhance the efficiency of ODS processes[6–8].

Wang *et al* carried out pore engineering by synthesizing amphiphilic hierarchical ZSM-5 using the bottom-up method, namely a synthetic method from the start where the hierarchical pore engineering process with a high Si/Al ratio was carried out during the synthesis process and impregnated with Ti[8]. Jafarinasab *et.al* impregnated Co into the mesopore imidazolate framework of zeolite-67 to form CoZIF-67, which was then modified again by pore engineering combined with HPMo encapsulation to become CoZIF-67[9,10]. Dashtpeyma *et al* modified the hierarchical clinoptilolite zeolite pores using a delamination-desilication modification method impregnated with $BiVO_4$-CuO[11]. Yao *et.al* carried out pore hierarchy engineering on meso-TS-1 zeolite treated with hydrophobization created by sequential pre-treatment, mesoporous-assisted DGC and hydroxyl radical post-treatment by increasing the amount of TIO_6 carried by the zeolite[12]. Kargar et.al synthesized the magnetic catalyst Fe_3O_4/ZIF-8/TiO_2 for the ODS process. The Fe catalyst's magnetic properties simplify the separation of ODS results. Nevertheless, the process still necessitates agent mass transfer and takes longer compared to the widely reported ODS process, which only takes 6 hours[13]. Zhang *et al* synthesized hierarchical pores with the help of amide into TS-1 zeolite and formed the active site Ti $(OH_2)_2(OH)_2(OSi)_2$[6]. However, most still use mass transfer agents such as acetonitrile to overcome the biphasic hindrance and use excess oxidant from stoichiometry resulting in large by-products. The H_2O_2 oxidant produces water, thereby increasing the water ratio in the fuel, while the TBHP oxidant, produces tertiary butanol which will reduce the quality of the fuel[5,14].

Several studies are concerned with exploring catalysts that can overcome problems in the ODS process and increase its effectiveness in terms of ease of synthesis, selectivity, and performance. The desired catalyst has mesopore-dominated hierarchical pores to facilitate the oxidation reaction of Dibenzothiophene (DBT) which has a large molecular size, around 9Å, and better reaction transport[15,16]. In addition, the hydrophobic nature of the catalyst helps overcome biphasic hindrance[12,17]. From a review of reported ODS research, Fe and Co are currently an attractive combination of transition metals in ODS processes[18–21]. Nie *et.al* discovered that combining transition metals Fe and Co in a 5:2 ratio yields the most optimal mixture. This combination generates a potent peroxidase enzyme, which efficiently breaks down H_2O_2, akin to a Fenton-like reaction. This reaction results in the creation of hydroxyl radicals, which can effectively oxidize organosulfur compounds. It is that this type of reaction is rarely reported[22].

Therefore, we propose a hierarchical strategy by engineering the ZSM-5 catalyst as a support for the Fe-Co ferromagnetic transition metal in a 2:1 ratio, which can create the Fe-Co/ZSM-5Hierarchy catalyst. This catalyst contains mainly mesopores and is hydrophobic, resulting in enhanced performance. In this study, we also evaluated the catalyst effectiveness on a DBT model diesel fuel in a solution of long-chain hydrocarbon compound, n-hexadecane, a unique approach that has not been previously reported in ODS process catalyst tests.

2. RESEARCH METHODS

Materials and Chemicals

The chemicals used include NaZSM-5, HF (hydrofluoride Acid) 48 %, $Co(NO_3)_2.6H_2O$ (Cobalt nitrate hexahydrate) ACS reagent 98 %, $Fe(NO_3)_3.9H_2O$ ACS reagent 98% (Iron (III) nitrate nonahydrate), NH_4Cl (Ammonium chloride) 99.5 %, Dibenzothiophene (DBT) 99 %, n-Hexadecane, $AgNO_3$ (Argentum nitrate) 2.5 %, H_2O_2 (Hydrogen peroxide) 30 wt. %, obtained from Merck Indonesia analytical pure without further purification. Aquadestillate prepared in Laboratory. A diesel model was prepared from DBT in n-Hexadecane.

Catalyst Preparation

NaZSM-5 Activation

500 mL of 1 M NH_4Cl solution was added to 40 grams of NaZSM-5, which was then refluxed for 5 h at a temperature of 900 ^oC. Afterward, NaZSM-5 was washed and filtered with distilled water 4 times until it was free of Cl^-, which was tested with $AgNO_3$. Then it was filtered and put in the oven set at 65 ^oC for 24 h. Next, it was calcined in a furnace at a temperature of 450 ^oC for 3 h[23,24].

Synthesis of HZSM-5 Hierarchy

HZSM-5 is the result of activation of NaZSM-5 which is then hierarchical by dealumination with 10 % HF added, then stirred until homogeneous for 30 min. Then filtered and washed with distilled water 3 times. Then steam treated with 1M NH_4Cl solution for 5 h at 90 ^oC. After that, it was filtered and washed three times until it was free of Cl^-, which was tested with an $AgNO_3$ solution. Next, it is dried in an oven for 8 h at a temperature of 100 ^oC, then calcined in a furnace at a temperature of 550 ^oC for 3 h[25,26].

Impregnation of ZSM-5

Following the dealumination of ZSM-5, the resultant material was wet impregnated with Fe-Co bimetal, with a 2:1 ratio of Fe to Co, at concentrations of 5% and 15%. The mixture was stirred for a period of three hours with the aid of a magnetic stirrer, after which it was subjected to an oven at a temperature of 50°C for a duration of 12 hours. Subsequently, it was calcined at a temperature of 450 °C for a period of 5 hours[27,28].

Catalyst Characterization

The resulting catalyst was then characterized using an XRD (X-Ray Diffraction) instrument, Rigaku Miflex on CuKα Monochromatic Radiation Beam (1.5405 Å) to identify the structure and determine crystallinity, with a speed of 10º/min and a range of 2θ 3-90º, and a step width 0.02º. Then the SAA (Surface Area Analyzer Quantacrome Nova 4200e) instrument with the BET (Brunauer Emmett-Teller) and BJH (Barret-Joiner-Halenda) methods to measure the N_2 adsorption-desorption isotherm and determine the surface area, pore volume, and pore diameter. Nitrogen adsorption and desorption isotherms were measured at 77 K in the relative pressure range of 0.05–0.99. X-ray fluorescence analysis (ED-XRF type) using Rigaku NexCG to determine the amount of metal in the catalyst.

Catalytic Oxidative Desulfurization of Model Oil

Put the catalyst into a three-neck flask, then add 10 mL of model oil, namely DBT in n-Hexadecane with a concentration of 500 ppm, and add 30 wt% H_2O_2 oxidant. The process is carried out with varied conditions to find optimum operating conditions. After the ODS process, the results are separated by decantation. The search for the conditions of the desulfurization oxidation process with the Fe-$Co_{(15)}$/ZSM-5 catalyst was carried out on DBT in n-hexadecane as a model oil at a concentration of 500 ppm for 10ml. This is done by varying the amount of catalyst according to the number of catalysts used in 10 mL of model oil, that is 0.05, 0.1, 0.2, 0.3 g, and varying the ratio of H_2O_2 as oxidant concentration used to DBT in model oil (O/ S); 1, 2, 4 .7, temperature variations 35, 45, 60 ºC, and time variations 30, 45, 60 min. The result that provides optimal DBT conversion is taken as the operating condition.

The amount of converted sulfur was determined using a UV-Vis instrument that had been calibrated for absorbance and a concentration geometric series search was carried out. Measurements were carried out with a Uv-Vis Spectrophotometer - Thermo Scientific Genesys 10 S spectrum at a wavelength of 320 nm. Next, the removal of sulfur compounds is calculated as a DBT conversion with the equation 1 [29–31]:

$$\text{DBT conversion} = \alpha = \frac{C_0 - C_i}{C_0} x\ 100\% \qquad (1)$$

Where:
C_0 = initial concentration of DBT
C_i = final concentration of DBT

Then the catalyst TOF (Turnover Frequency) is calculated in the oxidative desulfurization catalytic reaction with the equation 2 [6]:

$$\text{TOF} = \frac{\text{n(sulfide)initial x } \alpha}{\text{n}(Fe-Co) \times \text{ Reaction time}} \qquad (2)$$

Where n(sulfide)initial is the initial mole of sulfide, and n(Fe-Co) is the mole of Fe-Co species in the catalyst.

3. RESULTS AND DISCUSSION

Catalyst Characterization

The XRD pattern characterization confirmed the structural characteristics of Fe-Co/ZSM5-Hierarchy, as shown in Figure 1. Each pattern displays the typical Type MFI zeolite structure peak at the 2θ point at 8º-25º [32,33]. Which one, XRD instrument analysis matched the XRD pattern to ICDD (PDF2.DAT), with NaZSM-5, HZSM-5, and HZSM-5Hierarchy matching DB card number 00-037-0361, and Fe-$Co_{(5)}$/ZSM-5Hierarchy corresponding to DB card number 00-039-0161, phase name ZSM-5(Fe). Additionally, Fe-$Co_{(15)}$/ZSM-5Hierarchy matched DB card number 00-048-0134 with the phase name ZSM-8. While there was no significant change in peak position, there was a clear change in peak height, indicating the influence of each treatment (activation, dealumination, and impregnation treatments) given. Changes in peak height can be attributed to a decrease in atoms in the crystal structure, which can cause an increase in crystal size, while a decrease in peak height can be caused by an increase in atoms in the crystal structure or a decrease in crystal size[24,28,34].

It appears that the desired catalyst synthesis was successful as there was a noticeable change in the height of the diffraction peak from Na-ZSM-5 to H-ZSM-5 after the Na atom was removed. At the highest point of 2θ at 23º, there was a significant increase in 2θ at 8º. After dealumination, there was a notable increase in the peak, especially visible at the peak height of 2θ at 8º due to the loss of Al atoms from the dealumination process with hydrofluoric acid (HF). The high peak at 2θ at 8º suggests the presence of a mesoporous[35,36]. Moreover, when HZSM-5Hierarchy was impregnated with bimetal Fe-Co, there was a decrease in peak height, indicating that the loading of metal impregnated can affect the crystal size and crystallinity[37,38]. Metal impregnation generally decreases crystallinity and crystal size, but the type and amount of metal impregnated affects the strength. The heat given to HZSM-5 which has embedded metal, causes atomic shifts, convergence, or divergence of atoms freely. This can cause the crystal lattice to vibrate and probably phase changes to occur[39,40]. As previously explained, the results of the XRD instrument analysis stated that the Fe-Co(5)/ZSM-5Hierarchy catalyst matches the ZSM-5 (Fe) phase while the Fe-Co(15)/ZSM-5Hierarchy matches the ZSM-8 phase.

The XRD test results shown in Table 1 show that HZSM-5 impregnated with 5% bimetal Fe-Co (Fe-$Co_{(5)}$/ZSM-5Hierarchy) has the smallest crystal size.

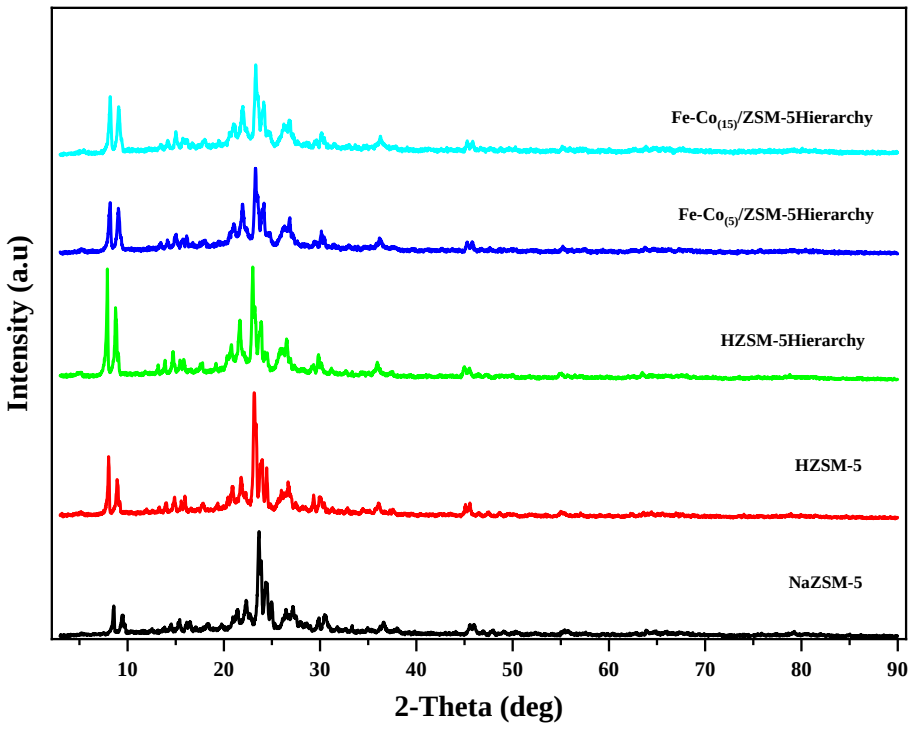

Figure 1. XRD Diffraction Pattern

Table 1. The Crystallinity and Crystallite Size

	Crystallinity (%)	Crystallite Size (Å)
NaZSM-5	19.6	131
HZSM-5	42	252
HZSM-5Hierarchy	52.2	239
Fe-Co$_{(5)}$/ZSM-5Hierarchy	31.5	36
Fe-Co$_{(15)}$/ZSM-5Hierarchy	38.8	190

Table 2. Elemental composition in catalysts based on XRF analysis

Catalyst	Si/Al ratio	Fe-Co Content (%)	
		Fe	Co
Fe-Co$_{(5\%)}$/HZSM-5Hierarchy	51.75	1.3	0.5
Fe-Co$_{(15\%)}$/HZSM-5Hierarchy	51.38	1.4	0.9

A sample with high crystallinity will produce a diffraction pattern with intense and sharp peaks. Conversely, an amorphous material will not have any peaks in its diffraction pattern. Table 1 illustrates the high crystallinity of the HZSM-5 hierarchy, and Figure 1 displays the highest peak at peak 2θ at 23°. The size of the crystals is determined by examining the main peaks in the diffraction pattern obtained from the XRD instrument test results. Using an approach Debye Scherrer's equation is formulated :

$$D = \frac{K\ \lambda}{\beta \cos\theta}$$

Where:
D = Crystal size
B = FWHM value
θ = Bragg angle
λ = wavelength of X-ray light.
K = constant "Shape Factor" (0.8-1)

The XRF test results in Table 2 show that more Fe-Co is embedded in the Fe-Co$_{(15)}$/ZSM-5Hierarchy, but the Fe: Co ratio is greater in the Fe-Co$_{(5)}$/ZSM-5Hierarchy catalyst. From Table 2, it can also be seen that the Si/Al ratio values are almost the same for the catalysts tested for the bimetal Fe-Co$_{(5)}$ and Fe-Co$_{(15)}$ embedded catalysts. It can be said that the catalyst used is close to homogeneous[41]. The dealumination process causes a high Si/Al ratio which makes the catalyst hydrophobic[7,42]. It is known that the Si species that influence the catalyst properties lead to hydrophobicity[43].

The BET analysis shows the N_2 adsorption and desorption isotherms shown in Figure 2 with its textural properties summarized in Table 3. According to the IUPAC classification, the sample shows that NaZSM-5 is a type I adsorption isotherm, where this type is usually obtained from adsorbents with micropores of less than

2nm and a small surface area[44,45]. As seen from Table 3, NaZSM-5 has the smallest surface area, namely 31.87 m^2/g. Then HZSM-5 has a pattern that is almost the same as NaZSM-5, with type I isotherm, but HZSM-5 has a hysteresis loop close to type IV. This is due to a shift in the position of Na which is replaced by H upon ZSM-5 activation, so that there is capillary condensation and evaporation at different pressures which causes a hysteresis loop. Meanwhile, for the HZSM-5 Hierarchy, Fe-$Co_{(5)}$/ZSM-5 Hierarchy, and Fe-$Co_{(15)}$/ZSM-5 Hierarchy catalysts, the type of catalyst adsorption isotherm is type IV, and the hysteresis loop is type IV[44]. Figure 2 also shows that The catalyst has pores or is a porous material with a relatively high absorption amount at P/Po ~ 0,933.37. N_2 adsorption on H-ZSM-5Hierarchy and Fe-$Co_{(15)}$/ZSM-5Hierarchy is significantly high at P/Po ~0.9 which reflects that the catalyst has a lot of mesopore structure[46].

Embedded metals to zeolites can increase surface area, increase catalytic active sites, and improve accessibility to reactants. However, the magnitude of this effect depends on several factors, including the type of metal used and the impregnation technique. Even distribution of the impregnated metal on the support is very important because uneven distribution can cause pore blockage and agglomeration. Supports with high porosity or dominated by mesopores are more likely to show an increase in surface area after metal impregnation[39,47–51].

Table 3 shows that the NaZSM-5 catalyst activation process can increase the surface area of the catalyst from 31.87 m^2/g to 150.85 m^2/g, but does not change the average pore radius. The activation process opens due to ion exchange between NH_4^+ ions and Na cations in Na-ZSM-5. This activation process is carried out by heating using NH_4^+, where on heating it will become NH_3 vapor and allow H^+ to bind to ZSM-5 to form H-ZSM-5. The loss of Na cations produces more templates or pores thereby increasing catalytic activity[23,32]. In contrast to dealumination, the dealumination process not only increases the catalyst surface area to 166 m^2/g in HZSM-5 Hierarchy but also increases the pore radius to 1,591 and clarifies the micro, meso, and macro pore levels with a high number of mesopores, so it can be said to be a hierarchical process succeed. The dealumination process to form a pore hierarchy is said to be successful when there are several levels of pores, signs of eliminating micropores[25,52]. The dealumination process collapses the structure of ZSM-5 and extracts Al species from the framework, thereby opening the pores. Dealumination is carried out by steam treatment using NH_4Cl to keep the main structure from collapsing but can open the pores with HF which extracts Al, this steam process helps form hydroxyl so that Si can replace Al's position in the framework optimally. Extracted Al from the skeleton[25,26]. Table 3 also shows that the surface area of the catalyst is maintained and even tends to increase after impregnation, namely to 191.18 m^2/g on Fe-$Co_{(5)}$/HZSM-5Hierarchy, and 168.94 on Fe-$Co_{(15)}$/HZSM-5Hierarchy, while maintaining the Pore hierarchy. The reduced surface area in the Fe-$Co_{(15)}$/HZSM-5 Hierarchy is probably caused by the impregnation process, most of the surface is covered or pore blockage by the high bimetal concentration, thereby reducing the pore surface area. The catalyst pore size distribution in Figure 3 shows that it is in the range of 1.4 to 60 nm with larger mesopores, namely r > 1 nm or d > 2 nm.

The results of the analysis of catalyst characteristics can be said to have succeeded in designing the mesopore-dominated Fe-Co/HZSM-5Hierarchy catalyst, which is expected to overcome the steric barrier of problems in the desulfurization process so far, because the size of the organosulfur molecules in the fuel is large, especially the DBT[10,53]. Then the hydrophobic nature of this catalyst can overcome the biphasic hindrance of the difference in polar poles of the ODS reaction[7,46]. The overcoming of steric barrier and biphasic hindrances causes the use of oxidant as O/S following the stoichiometric amount of 2 mol so that it does not cause interference from the formation of large amounts of aqueous from the decomposition of oxidant, thus increasing the effectiveness of the catalyst[5,54.]

Table 3. Physicochemical properties of the catalyst

Catalyst	[a]Surface area (m^2/g)	[b]Pore radius avg (nm)	[C]Micro pore Volume (cc/g)	[d]Meso pore Volume (cc/g)	[e]Macro pore Volume (cc/g)
NaZSM-5	31.87	1.483	0.012	0.0278	0.0005
HZSM-5	150.85	1.483	0.055	0.0267	0.0002
HZSM-5Hierarchy	166.26	1.591	0.060	0.0720	0.0010
Fe-$Co_{(5)}$/HZSM-5Hierarchy	191.18	1.591	0.060	0.0460	0.0002
Fe-$Co_{(15)}$/HZSM-5Hierarchy	168.94	1.591	0.062	0.0777	0.0010

[a]Surface area and was determined by BET analysis.
[b,c,d,e]Pore radius average, micro, meso, and macro pore volume were determined by the BJH adsorption-desorption curve.

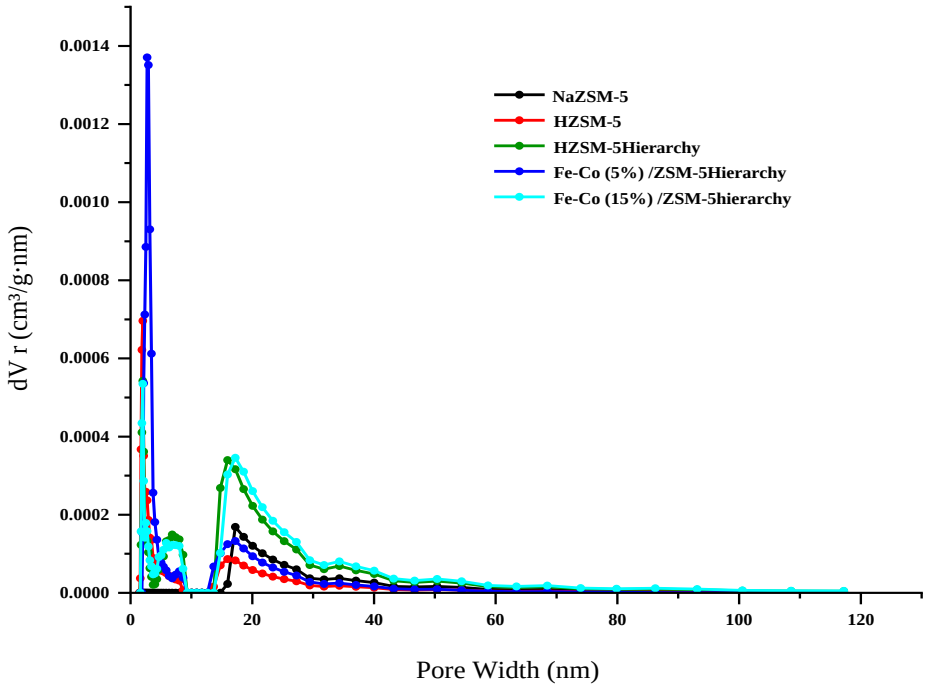

Figure 3. Catalyst pore distribution

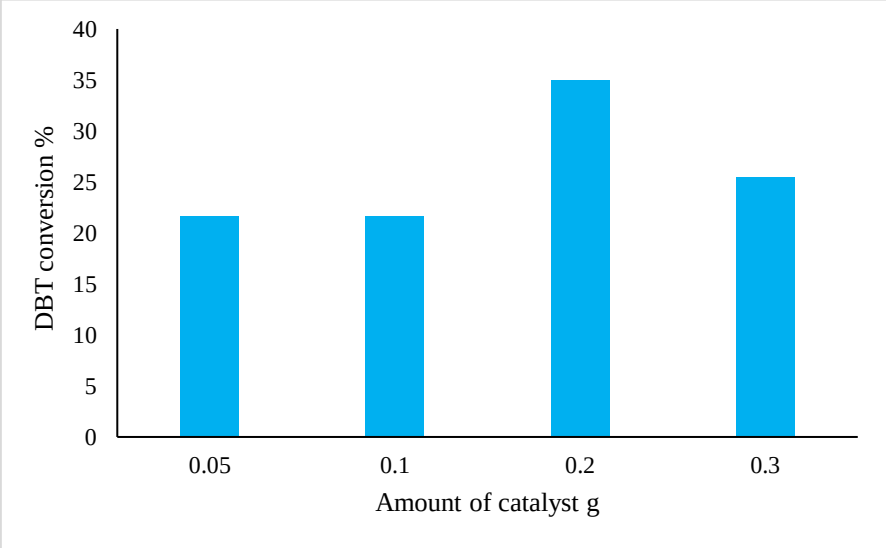

Figure 4. Effect the amount of catalyst on the ODS process with Fe-$Co_{(15)}$/ZSM-5Hierarchy catalyst

Catalytic Oxidative Desulfurization of Model Oil
Looking for ODS operating conditions

Looking for ODS operating conditions on model oil with the Fe-$Co_{(15)}$/ZSM-5Hierarchy catalyst because it is considered to have a larger amount of Fe-Co, so it can produce enough hydroxyl to oxidize organosulfur properly so that large conversions can be obtained. look for operating conditions with a 10 ml oil model with variations in the amount of catalyst, oxidant ratio with DBT concentration in fuel [O/S], temperature variations, and time variations. Then the results of the optimum operating conditions obtained were applied to the Fe-$Co_{(5)}$/ZSM-5Hierarchy, HZSM-5Hierarchy, HZSM-5, and NaZSM-5 catalysts**.**

Effect the amount of catalyst

The amount of catalysts here is the amount of catalysts used in the ODS process. Figure 4 shows a trend of significantly increasing conversion at a catalyst amount of 0.2 g and decreasing when the amount exceeds 0.2 g. This shows that catalysts play an important role in the ODS process. This means that at that dose, the catalyst offers a sufficient amount of active sites for high catalytic reactivity. If there are excess active sites, collisions with reactants will not be effective, resulting in a decrease in reaction yield. In addition, excess catalyst causes competing reactions to occur with active species and affects the reaction equilibrium, resulting in reduced catalyst activity[55,56].

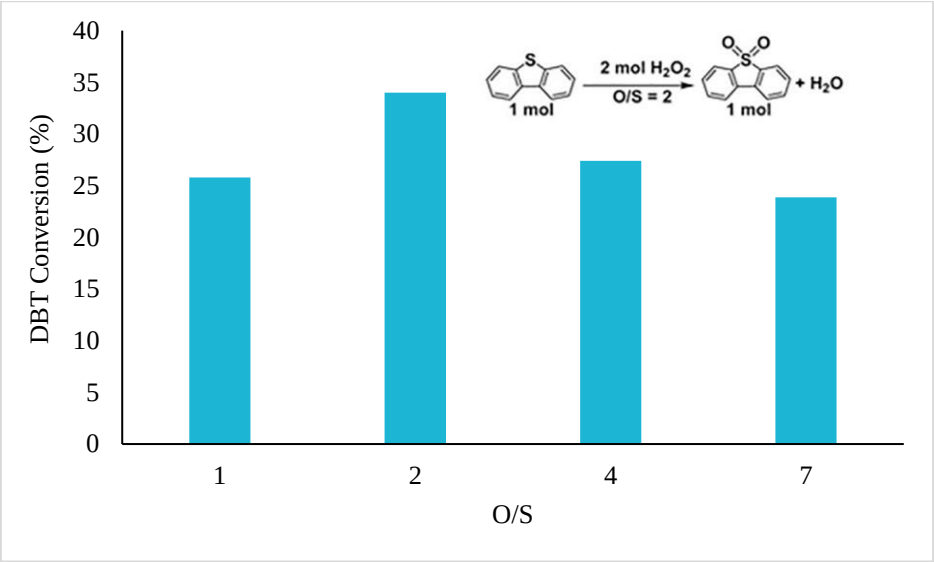

Figure 5. Effect of oxidant ratio on the ODS process with the Fe-$Co_{(15)}$/ZSM-5Hierarchy catalyst

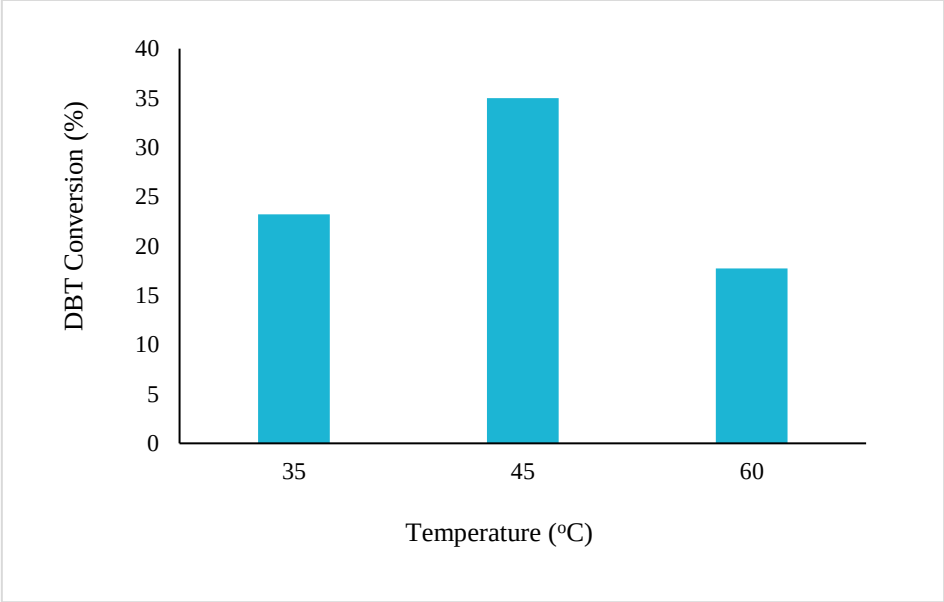

Figure 6. Effect of temperature on the ODS process with the Fe-$Co_{(15)}$/ZSM-5Hierarchy catalyst

Effect of Oxidants (O/S)

The oxidant ratio refers to the proportion of oxidant utilized to the sulfur concentration present in the fuel. As illustrated in Figure 5, the highest conversion can be achieved when the O/S ratio is at 2. This indicates that the optimum conditions for the O/S ratio, as per stoichiometry, have been attained. Any addition of oxidant beyond stoichiometry has a negative effect since it significantly reduces conversions. The oxidant H_2O_2, used to oxidize DBT, produces water as a by-product. However, excess water can make it challenging for oxidant reactions to occur with species at the active site of the catalyst[6,7,55]. The type of catalyst has a significant impact on the ability of oxidants to oxidize. Impregnated Fe-Co aims to enhance the decomposition of H_2O_2 oxidants, thereby generating abundant molecular oxygen to ensure optimal organosulfur oxidation in fuel. Figure 5 demonstrates that the objective of Fe-Co impregnation is achieved by utilizing oxidants at stoichiometry O/S 2. Scheme 1 depicts the mechanism of bimetal Fe-Co decomposition of H_2O_2.

Effect of Temperature

The ODS process offers several appealing advantages, notably its ability to function under mild operating conditions that are considerably lower than traditional HDS processes[57]. During this process, temperature aids polar oxidants in penetrating the pores of the hydrophobic catalyst, which has been effectively dispersed within the non-polar model oil. This allows for reactions to take place effectively on the pore surface[7,8]. As depicted in Figure 6, DBT conversion rates steadily rise with increased temperature but begin to decline gradually beyond 45°C. This may be because H_2O_2 is prone to decomposition at high temperatures, leading to premature oxidant breakdown and subsequent disruption

in the reaction equilibrium caused by the presence of excess oxidants. The outcome of the H_2O_2 decomposition reaction is determined by contact with the active site, which can generate other reactions that interfere with the oxidation reaction, ultimately resulting in a decreased DBT conversion[56].

Effect of Time

Reaction time follows the reaction pattern and the nature of the reaction to factors that influence the reaction such as temperature, amount of reactant, and catalyst[6,58]. In this study, reaction times varied at 30, 45, and 60 min, and Figure 7 shows that the optimum reaction occurred at 45 min, which means the reaction rate was large at this time and decreased after passing the reaction equilibrium. Figure 7 shows that as time increases, the conversion decreases and it can be seen that the trend of the time-influence phenomenon is close to the temperature-influence trend.

ODS Catalytic Process

The Fe-Co/ZSM-5Hierarchy catalyst effectiveness test was carried out with model oil, namely DBT in Hexadecane with a concentration of 500 ppm. The ODS process was carried out under optimum conditions, namely at a temperature of 45°C, with the amount of catalyst used in the process being 0.2 g, O/S 2, and a reaction time of 45 min. Figure 8 shows that engineering the pores into a hierarchy has a big influence on the ODS process, where it can be seen that the DBT conversion increases significantly. Then the increase continued to occur on the catalyst that had been embedded with bimetal Fe-Co, with the highest DBT conversion on the Fe-$Co_{(5)}$/ZSM-5Hierarchy catalyst, with a TOF value of 205 h^{-1} (equation 2). Decreased DBT conversion on the Fe-$Co_{(15)}$/ZSM-5Hierarchy catalyst with a TOF value of 157 h^{-1}. This means that Fe-$Co_{(5)}$/ZSM-5Hierarchy is a promising catalyst and provides high reactivity for the ODS process with a sufficient number of active sites. It can also be said that high catalyst reactivity occurs in catalysts that have a higher Fe: Co active site ratio.

Measuring the TOF (turnover frequency) value is a determining parameter for catalyst performance. TOF is the number of moles of reactant converted to the desired product by each active site per hour. This is calculated from the reaction rate and the amount of active site metal (equation 2), which can be said to directly measure the reaction productivity and active site reactivity of the catalyst[6,59]. TOF is a measure of the intrinsic activity of a catalyst which is an important parameter in catalyst science that functions to measure the number of reactions that can be carried out by one active site in a catalyst per certain unit of time. The TOF value is used to determine the efficiency and performance of catalysts in various reactions by providing an overview of the reaction speed at the molecular level at the active site of the catalyst. This is important to understand because TOF can provide insight into how quickly a catalyst can catalyze a particular reaction, which in turn can influence the efficiency of the overall catalysis process[6,60]. This means that the Fe-Co/ZSM-5Hierarchy catalyst has great potential in the ODS process so it is interesting to continue to explore it to produce higher catalyst activity so that ultra-low desulfurization can be achieved.

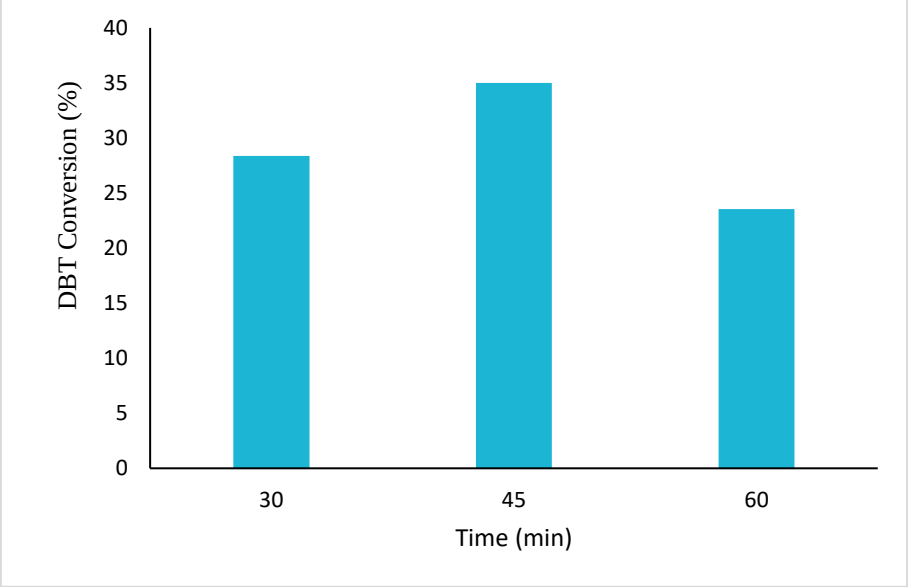

Figure 7. Effect of time on the ODS of the process with the Fe-$Co_{(15)}$/ZSM-5Hierarchy catalyst

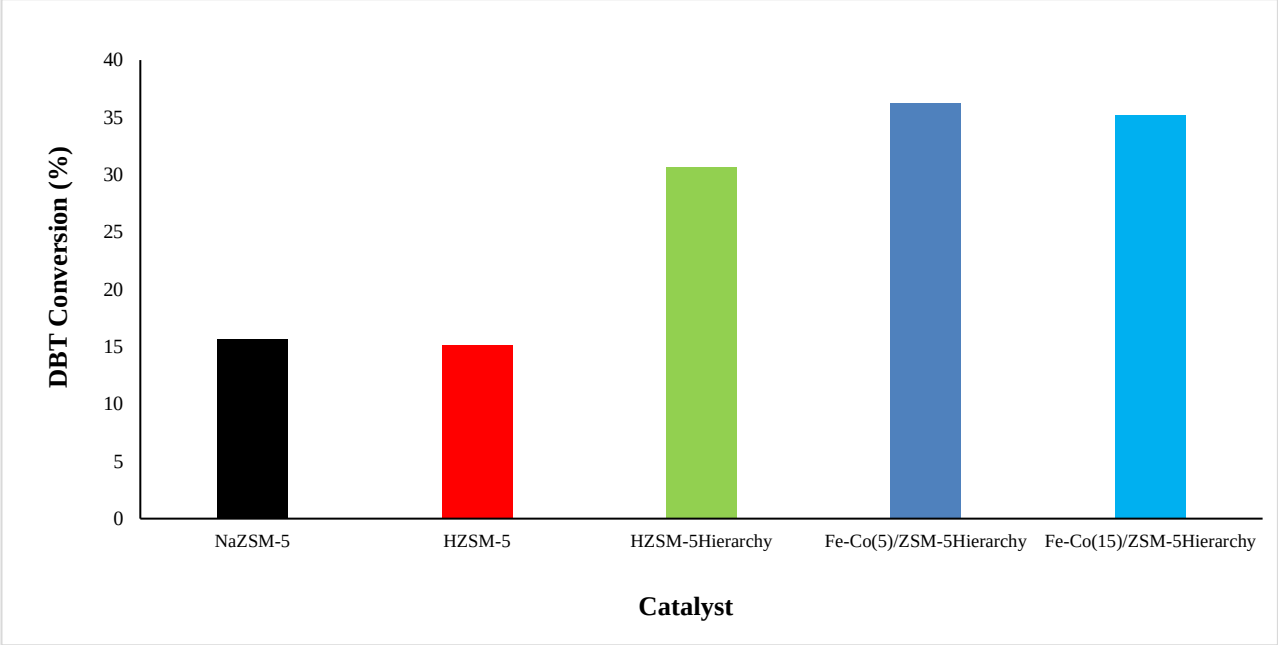

Figure 8. Catalytic Oxidative Desulfurization Process of 10 mL DBT in n-Hexadecane, concentration of 500 ppm at optimum conditions, i.e. temperature 45 ºC, time 45 minutes, O/S = 2, amount of catalyst 0.2 g

Table 4. Comparison of TOF dari proses ODS DBT from recent reports with various catalysts

DBT in (Model Oil)	Catalyst	Synthesis method	O/S Oxidant	Condition	TOF (h^{-1})	Reff
n-Octane	Amide-assisted-$Ti(OH_2)_2(OH)_2(OSi)_2$-zeolites (AM-TS-95)	Synthesis with the bottom up methode	4 (TBHP)	60 ºC 30 mnt	134.8 initial concentration300 ppm	[6]
Model oil	Co@C/P-5 (advanced material MOF)	-	7.5 (H_2O_2)	60 ºC 60 mnt	104	[59]
n-Hexadecane	Fe-$Co_{(5)}$/ZSM-5Hierarchy	Top-down dealumination with wet impregnation	2 (H_2O_2)	45 ºC 45 mnt	205	This work
	Fe-$Co_{(15)}$/ZSM-5Hierarchy				157 initial concentration500 ppm	

Table 4 shows the comparison of TOF values using similar ODS methods. It can be seen that the Fe-Co/ZSM-5Hierarchy catalyst has a higher TOF value in the DBT process on long-chain model oil, with the use of an oxidant according to its stoichiometry, without the addition of mass transfer agents or extractants. This means that the Fe-Co/ZSM-5 Hierarchy catalyst is a promising catalyst for the ODS process and is interesting to continue to explore.

Proposed Reaction mechanism

The proposed ODS mechanism presented in Figure 9 will demonstrate the catalytic role of Fe-Co/ZSM-5Hierarchy in the Dibenzothiophene ODS process. The ferromagnetic nature of Fe-Co bimetal will stop the organosulfur resonance in the fuel, thereby facilitating the electron transfer process in the ODS process[17,61]. The hydrophobic nature of the catalyst overcomes the biphasic barrier, thus facilitating the dispersion of the catalyst in the fuel and the entry of organosulfur into the catalyst pores to react with oxidants at their optimum temperature[7,8]. *OH radicals are real oxidants that oxidize S compounds to sulfoxides, and finally sulfones[56,62]. *OH radicals are produced from the decomposition of H_2O_2 as an oxidant which is produced in three ways in the decomposition process with bimetal Fe-Co which is shown in scheme 1. Firstly, bimetal Fe-Co donates electrons to H_2O_2 so that decomposition occurs which produces *OH radicals. Then hydrolysis occurs of the Fe^{3+} and Co^{3+} to become Fe^{2+} and Co^{2+} and *OOH radicals are produced at the same time. Next, the *OOH radical forms the *OH radical through a bimolecular self-reaction by releasing oxygen[20,63]. The redox cycles of Fe^{3+}/Fe^{2+} and Co^{3+}/Co^{2+} promote the

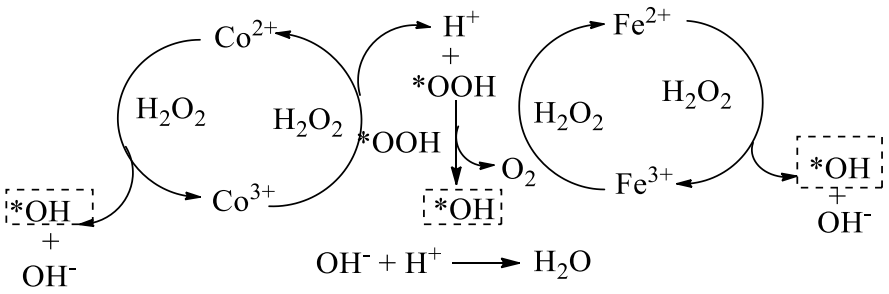

Scheme 1. Reaction mechanism of H_2O_2 decomposition by the active site of the Fe-Co/ZSM-5Hierarchy catalyst

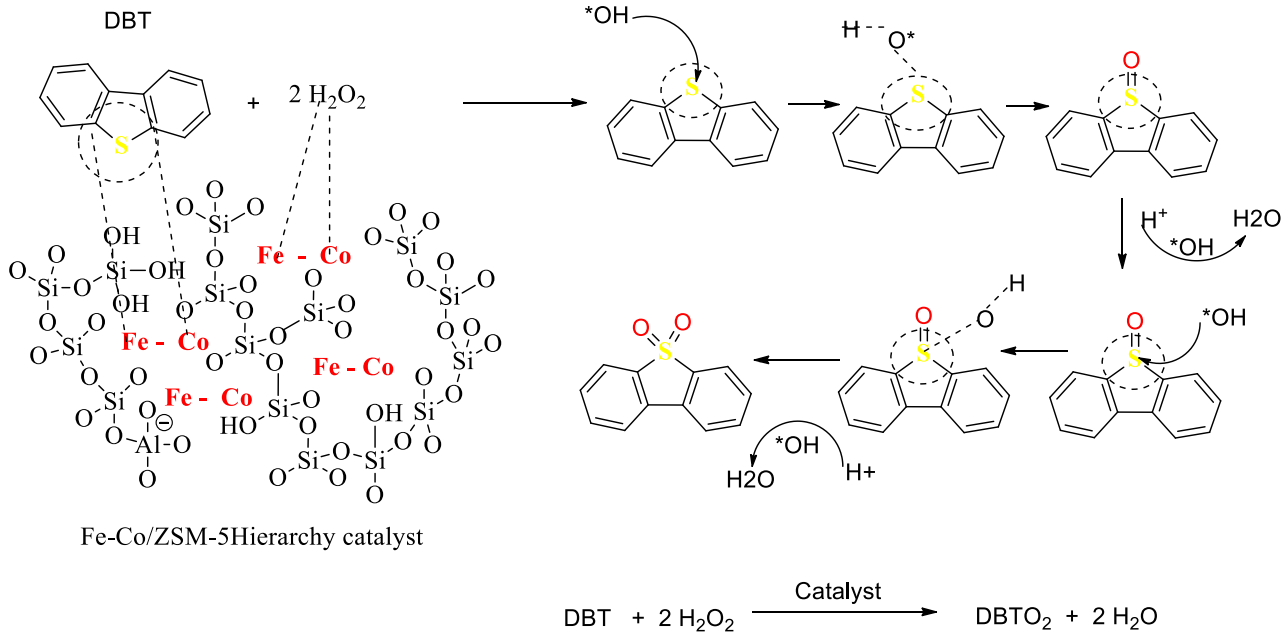

Figure 9. Proposed reaction mechanism of ODS dibenzothiophene by Fe-Co/ZSM-5Hierarchy catalyst

continuous formation of *OH radicals. In the end, the Fe-Co/HZSM-5Hierarchy returns to its original form, where the framework is porous and hydrophobic, causing the sulfones and water produced to be trapped by the framework so that the model oil is very easily separated by decantation[8]. This shows that the reaction easily occurs on the active site of Fe-Co/ZSM-5Hierarchy. In theory, it is known that the ODS reaction occurs in two stages, namely the sulfoxide formation stage followed by the formation of sulfone[64]. This is one of the reasons why sulfone oxidation is often less successful because the sulfoxide formation step is a nucleophilic event that requires electron transfer facilities from nucleophilic species[64,65]. In fact, in theory, the oxidation reaction of organosulfur compounds is an electrophilic substitution reaction that requires electrophile species. Here, Co^{2+}/Co^{3+} is responsible for facilitating the formation of sulfoxide very quickly by removing the hydrogen atom from the organosulfur group and replacing it with oxygen from the hydroxyl radical as a nucleophile species so that the sulfoxide formation reaction is easily passed[18,54,66]. Then electrophilic substitution to form products occurs easily because of the presence of reactive oxygen as an electrophile species from the breakdown of *OOH which results from the decomposition of H_2O_2 by Fe-Co. HOO* is a hydroxyl peroxide radical, i.e. a molecule with one unpaired electron, so it is very reactive and the presence of Fe-Co allows it to participate in reactions that produce electrophilic oxygen[20,63,67,68].

4. CONCLUSIONS

The Fe-Co/ZSM-5Hierarchy catalyst has been successfully obtained which is dominated by mesopores and has hydrophobic and environmentally friendly properties. The characteristics of the catalyst show that the hierarchical process using a top-down dealumination method with steam treatment under reflux conditions on the HZSM-5 catalyst support causes the catalyst to have multimodal pores dominated by mesopores with a high surface area so that it can overcome steric barrier in the Dibenzothiophene ODS process. Catalyst reactivity is characterized by the TOF value, where Fe-$Co_{(5)}$/ZSM-5Hierarchy has the highest TOF value of 205 h^{-1} under mild operating conditions, namely 45° C, for 45 min with oxidant at an O/S ratio according to stoichiometry, namely 2 and the amount of catalyst used is 0.2 g. Apart

from that, the catalyst has a high Si/Al ratio, causing the catalyst to be hydrophobic, where this hydrophobic property can overcome the biphasic hindrance in the ODS DBT process on fuel, thereby increasing the effectiveness of the catalyst.

ACKNOWLEDGMENTS

The authors thank Universitas Bhayangkara Jakarta Raya for financial and laboratory support, as Ditjen Dikti for supporting the 2023 PTUPT Grant.

REFERENCES

1. Barker J, Reid J, Wilmot E, et al. Investigations of Diesel Injector Deposits Characterization and Testing. In: *SAE Technical Papers Series*.; 2020:21. doi:10.4271/2020-01-2094
2. Houda S, Lancelot C, Blanchard P, Poinel L, Lamonier C. Oxidative desulfurization of heavy oils with high sulfur content: A review. *Catalysts*. Published online 2018. doi:10.3390/catal8090344
3. Godin K, Sapinski JP, Dupuis S. The transition to net zero energy (NZE) housing: An integrated approach to market, state, and other barriers. *Cleaner and Responsible Consumption*. Published online 2021. doi:10.1016/j.clrc.2021.100043
4. Manab Idris A, Sasongko N, Kuntjoro Y. Energy Conversion and Conservation Technology in Facing Net Zero-Emission Conditions and Supporting National Defense. *Trends in Renewable Energy*. Published online 2022. doi:10.17737/tre.2022.8.1.00139
5. Rajendran A, Cui TY, Fan HX, Yang ZF, Feng J, Li WY. A comprehensive review on oxidative desulfurization catalysts targeting clean energy and environment. *J Mater Chem A Mater*. 2020;85(5):2246-2285. doi:10.1039/c9ta12555h
6. Zhang J, Bai R, Feng Z, Li J. Amide-assisted synthesis of TS-1 zeolites with active Ti(OH2)2(OH)2(OSi)2 sites toward efficient oxidative desulfurization. *Appl Catal B*. 2024;342:123339. doi:10.1016/j.apcatb.2023.123339
7. Zhu Z, Ma H, Liao W, et al. Insight into tri-coordinated aluminum dependent catalytic properties of dealuminated Y zeolites in oxidative desulfurization. *Appl Catal B*. 2021;288(February):120022. doi:10.1016/j.apcatb.2021.120022
8. Wang Y, Sun C, Wang R, et al. Preparation of Amphiphilic Ti/ZSM-5 Zeolite and Its Catalytic Performance in Oxidative Desulfurization. *Gaodeng Xuexiao Huaxue Xuebao/Chemical Journal of Chinese Universities*. 2019;40(6):1265-1270. doi:10.7503/cjcu20180770
9. Jafarinasab M, Akbari A, Omidkhah M, Shakeri M. An Efficient Co-Based Metal-Organic Framework Nanocrystal (Co-ZIF-67) for Adsorptive Desulfurization of Dibenzothiophene: Impact of the Preparation Approach on Structure Tuning. *Energy and Fuels*. 2020;34(10):12779-12791. doi:10.1021/acs.energyfuels.0c01888
10. Jafarinasab M, Akbari A. Co-ZIF-67 encapsulated phosphomolybdic acid as a hybrid catalyst for deep oxidative desulfurization. *J Environ Chem Eng*. 2021;9(6):106472. doi:10.1016/j.jece.2021.106472
11. Dashtpeyma G, Shabanian SR. Efficient photocatalytic oxidative desulfurization of liquid petroleum fuels under visible-light irradiation using a novel ternary heterogeneous BiVO4-CuO/modified natural clinoptilolite zeolite. *J Photochem Photobiol A Chem*. 2023;445:115024. doi:10.1016/j.jphotochem.2023.115024
12. Yao Y, Yang Z, Zheng P, Diao Z. Enhancing the accessible TiO6 concentration and the hydrophobicity of hierarchical TS-1 zeolites for alkene epoxidation and oxidative desulfurization. *Chemical Engineering Journal*. 2023;475. doi:10.1016/j.cej.2023.146053
13. Kargar H, Ghahramaninezhad M, Shahrak MN, Balula SS. An Effective Magnetic Catalyst for Oxidative Desulfurization of Model and Real Fuels: Fe3O4/ZIF-8/TiO_2. *Microporous and Mesoporous Materials*. 2021;317(October 2020):110992. doi:10.1016/j.micromeso.2021.110992
14. Tugrul Albayrak A, Tavman A. Sono-oxidative desulfurization of fuels using heterogeneous and homogeneous catalysts: A Comprehensive Review. *Ultrason Sonochem*. Published online 2021:105845. doi:10.1016/j.ultsonch.2021.105845
15. Yang G, Han J, Liu Y, Qiu Z, Chen X. The synthetic strategies of hierarchical TS-1 zeolites for the oxidative desulfurization reactions. *Chin J Chem Eng*. 2020;28(9):2227-2234. doi:10.1016/j.cjche.2020.06.026
16. Hartmann M, Thommes M, Schwieger W. Hierarchically-Ordered Zeolites: A Critical Assessment. *Adv Mater Interfaces*. 2021;8(4, 2001841):1-38. doi:10.1002/admi.202001841
17. Chen L, Yuan ZY. Design strategies of supported metal-based catalysts for efficient oxidative desulfurization of fuel. *Journal of Industrial and Engineering Chemistry*. 2022;108:1-14. doi:10.1016/j.jiec.2021.12.025
18. Song Y, Bai J, Jiang S, et al. Co-Fe-Mo mixed metal oxides derived from layered double hydroxides for deep aerobic oxidative

desulfurization. *Fuel*. 2021;306(1-2):121751. doi:10.1016/j.fuel.2021.121751

19. Rezvani MA, Maleki Z. Facile synthesis of inorganic–organic Fe 2 W 18 Fe 4 @NiO@CTS hybrid nanocatalyst induced efficient performance in oxidative desulfurization of real fuel. *Appl Organomet Chem*. Published online 2019. doi:10.1002/aoc.4895
20. Naghavi M, Mazloom G, Akbari A, Banisharif F. Deep oxidative desulfurization by sulfated alumina catalyst using ferrate (Fe(VI)) oxidant derived from scrap iron. *Chemical Engineering Research and Design*. 2021;174:454-462. doi:10.1016/j.cherd.2021.08.029
21. Eseva E, Dunko A, Latypova S, et al. Cobalt-manganese spinel structure catalysts for aerobic oxidative desulfurization. *Fuel*. 2024;357. doi:10.1016/j.fuel.2023.129689
22. Nie L, Li S, Gao X, et al. Sensitive visual detection of norfloxacin in water by smartphone assisted colorimetric method based on peroxidase-like active cobalt-doped Fe3O4 nanozyme. *J Environ Sci (China)*. 2025;148:198-209. doi:10.1016/j.jes.2023.12.022
23. Pereira Roldão C. Synthesis and comparative evaluation of HZSM-5 and NaZSM-5 zeolites in the catalytic dehydration of glycerol. Published online 2024. doi:10.21203/rs.3.rs-3940676/v1
24. Krisnandi YK, Nurani DA, Agnes A, et al. Hierarchical MnOx/ZSM-5 as heterogeneous catalysts in conversion of delignified rice husk to levulinic acid. *Indonesian Journal of Chemistry*. Published online 2019. doi:10.22146/ijc.28332
25. Qin Z, Shen W, Zhou S, et al. Defect-assisted mesopore formation during Y zeolite dealumination: The types of defect matter. *Microporous and Mesoporous Materials*. 2020;303:110248. doi:10.1016/j.micromeso.2020.110248
26. Xue YF, Niu YL, Zheng HY, et al. Selective dealumination of ZSM-5 by steaming and its effect on ethanol to propene. *Ranliao Huaxue Xuebao/Journal of Fuel Chemistry and Technology*. 2021;49(8):1111-1121. doi:10.1016/S1872-5813(21)60064-6
27. Aziz I, Adhani L, Maulana MI, Ali Marwono M, Dwiatmoko AA, Nurbayti S. Conversion of Nyamplung Oil into Green Diesel through Catalytic Deoxygenation using NiAg/ZH Catalyst. *Jurnal Kimia Valensi*. 2022;8(2):240-250. doi:10.15408/jkv.v8i2.25943
28. Adhani L, Fauzi A, Navanti D, Sri T. Rietveld Refinement Analysis of Lampung Natural Zeolite Catalyst Impregnated Fe with Diffraction Method Using MAUD Software. 2023;13(1).
29. Muhammad Y, Shoukat A, Rahman AU, Rashid HU, Ahmad W. Oxidative desulfurization of dibenzothiophene over Fe promoted Co–Mo/Al2O3 and Ni–Mo/Al2O3 catalysts using hydrogen peroxide and formic acid as oxidants. *Chin J Chem Eng*. Published online 2018. doi:10.1016/j.cjche.2017.05.015
30. Rachmawati DE, Susanto BH, Nasikin M. The effect of cerium promoted on Ni-Mo/Al2O3in oxygen adsorption isotherm and oxidative desulfurization study. In: *AIP Conference Proceedings*. Vol 2827. American Institute of Physics Inc.; 2023:1-7. doi:10.1063/5.0166127
31. Beshtar M, Khorasheh F, Larimi A, Akbar Asgharinezhad A. Photocatalytic oxidative desulfurization of model fuel using iron-molybdenum nanocatalyst based on cerium oxide (FeyMox/CeO2) under visible light. *Fuel*. 2024;360(6):130549. doi:10.1016/j.fuel.2023.130549
32. Krisyuningsih Krisnandi Y, Arifa Nurani D, Reza M, et al. Partial Oxidation of Methane to Methanol on Cobalt Oxide-Modified Hierarchical ZSM-5. In: *Biogas - Recent Advances and Integrated Approaches*. IntechOpen; 2021. doi:10.5772/intechopen.86133
33. Servatan M, Ghadiri M, Yazdi MK, et al. Synthesis of Cost-Effective Hierarchical MFI-Type Mesoporous Zeolite: Introducing Diatomite as Silica Source. *Silicon*. Published online 2021. doi:10.1007/s12633-020-00786-7
34. Liu Y, Shen J, Lu Z, Shen B, Yan L. Powder x-ray diffraction and Rietveld analysis of (C2H5NH3)2CuCl4. *Chinese Physics B*. Published online 2021. doi:10.1088/1674-1056/abee0a
35. Nqakala L, Mohiuddin E, Mpungose P, Mdleleni M. Effective hierarchical ZSM-5 catalysts for the cracking of naphtha and waste tire-derived oil to light olefins. *Biofuels, Bioproducts and Biorefining*. Published online 2024. doi:10.1002/bbb.2608
36. Mohiuddin E, Mdleleni MM, Key D. Catalytic cracking of naphtha: The effect of Fe and Cr impregnated ZSM-5 on olefin selectivity. *Appl Petrochem Res*. 2018;8(2):119-129. doi:10.1007/s13203-018-0200-2
37. Rostamizadeh M, Sadatnia B, Norouzbahari S, Ghadimi A. Enhancing the gas separation properties of mixed matrix membranes via impregnation of sieve phases with metal and nonmetal promoters. *Sep Purif Technol*. Published online 2020. doi:10.1016/j.seppur.2020.116859
38. Bemis R, Heriyanti, Sari RDP, Pratiwi N, Putri LFA. Synthesis and Characterization of Hydroxyapatite-Ag Nanocomposites Using Areca Nut Peel Bioreductors (Areca catechu L.)

for Antibacterial Applications. *Jurnal Kimia Valensi*. 2023;9(2):216-223. doi:10.15408/jkv.v9i2.32638

39. Sihombing JL, Herlinawati H, Pulungan AN, Simatupang L, Rahayu R, Wibowo AA. Effective hydrodeoxygenation bio-oil via natural zeolite supported transition metal oxide catalyst. *Arabian Journal of Chemistry*. 2023;16(50, 104707):1-14. doi:10.1016/j.arabjc.2023.104707
40. Mohamad Dzol MAA, Balasundram V, Shameli K, Ibrahim N, Manan ZA, Isha R. Catalytic pyrolysis of high-density polyethylene over nickel-waste chicken eggshell/HZSM-5. *J Environ Manage*. 2022;324. doi:10.1016/j.jenvman.2022.116392
41. Aziz I, Sugita P, Darmawan N, Dwiatmoko AA, Rustyawan W. Hydrodeoxygenation of palm fatty acid distillate (PFAD) over natural zeolite-supported nickel phosphide catalyst: Insight into Ni/P effect. *Case Studies in Chemical and Environmental Engineering*. 2024;9. doi:10.1016/j.cscee.2023.100571
42. Peron D V., Zholobenko VL, de Melo JHS, et al. External surface phenomena in dealumination and desilication of large single crystals of ZSM-5 zeolite synthesized from a sustainable source. *Microporous and Mesoporous Materials*. Published online 2019. doi:10.1016/j.micromeso.2019.05.033
43. Ismail A, Saputri LNMZ, Dwiatmoko AA, Susanto BH, Nasikin M. A facile approach to synthesis of silica nanoparticles from silica sand and their application as superhydrophobic material. *Journal of Asian Ceramic Societies*. 2021;9(2):665-672. doi:10.1080/21870764.2021.1911057
44. Sotomayor F, Quantatec AP, Thommes M, Sotomayor FJ, Cychosz KA. *Characterization of Micro/Mesoporous Materials by Physisorption: Concepts and Case Studies*. Vol 3.; 2018. https://www.researchgate.net/publication/331260891
45. Schlumberger C, Thommes M. Characterization of Hierarchically Ordered Porous Materials by Physisorption and Mercury Porosimetry—A Tutorial Review. *Adv Mater Interfaces*. 2021;8(4, 2002181):1-25. doi:10.1002/admi.202002181
46. Li L, Wang W, Huang J, et al. Synthesis of hydrophobic nanosized hierarchical titanosilicate-1 zeolites by an alkali-etching protocol and their enhanced performance in catalytic oxidative desulphurization of fuels. *Appl Catal A Gen*. 2022;630. doi:10.1016/j.apcata.2021.118466
47. Cieśla J, Franus W, Franus M, et al. Environmental-friendly modifications of zeolite to increase its sorption and anion exchange properties, physicochemical studies of the modified materials. *Materials*. 2019;12(19, 3213):1-13. doi:10.3390/ma12193213
48. Ejsmont A, Lewandowska-Andralojc A, Goscianska J. From Co-MOF to Co@carbon–comparison of needle-like catalysts in photo-driven hydrogen evolution. *Int J Hydrogen Energy*. 2024;67:704-714. doi:10.1016/j.ijhydene.2024.04.192
49. Visiamah F, Trisunaryanti W, Triyono. Microwave-assisted coconut wood carbon-based catalyst impregnated by Ni and/or Pt for bio-jet fuel range hydrocarbons production from Calophyllum inophyllum L. oil using modified-microwave reactor. *Case Studies in Chemical and Environmental Engineering*. 2024;9. doi:10.1016/j.cscee.2024.100722
50. Triyono. *EFFECT OF IMPREGNATION PROCEDURE OF Pt/γ-Al 2 O 3 CATALYSTS UPON CATALYTIC OXIDATION OF CO*. Vol 2.; 2002.
51. Susmanto P, Gusman Y, Ridwan MF, Tanara EH. CHARACTERIZATION OF Cr / SiO2 / AL2O3 CATALYST FROM RICE HUSK USING IMPREGNATION METHOD. *IJCA (Indonesian Journal of Chemical Analysis)*. 2020;3(1). doi:10.20885/ijca.vol3.iss1.art5
52. Peréz-Ramírez J, Verboekend D, Bonilla A, Abelló S. Zeolite catalysts with tunable hierarchy factor by pore-growth moderators. *Adv Funct Mater*. 2009;19(24):3972-3979. doi:10.1002/adfm.200901394
53. Mjalli FS, Ahmed OU, Al-Wahaibi T, Al-Wahaibi Y, AlNashef IM. Deep oxidative desulfurization of liquid fuels. *Reviews in Chemical Engineering*. 2014;30(4):337-378. doi:10.1515/revce-2014-0001
54. Xu H, Niu A, Yang Z, et al. Preparation of cobalt-containing polyvinylimidazole ionic liquid catalyst and coupling with persulfate for room-temperature ultra-deep desulfurization. *Fuel*. 2023;334. doi:10.1016/j.fuel.2022.126762
55. Rajendran A, Fan HX, Cui TY, Feng J, Li WY. Octamolybdates containing MoV and MoVI sites supported on mesoporous tin oxide for oxidative desulfurization of liquid fuels. *J Clean Prod*. 2022;334. doi:10.1016/j.jclepro.2021.130199
56. Fang Z, Zhao Z, Li N, et al. Low-temperature catalytic oxidative desulfurization by two-phase system with O-bridged diiron perfluorophthalocyanine. *Fuel*. 2021;306(July):121649. doi:10.1016/j.fuel.2021.121649
57. Campos-Martin JM, Capel-Sanchez MC. Catalytic Oxidative Desulfurization of Liquid Fuels. In: *ACS Symposium Series*. Vol 1379. American Chemical Society; 2021:143-174.

doi:10.1021/bk-2021-1379.ch006
58. Nikmanesh H, Jaberolansar E, Kameli P, Varzaneh AG, Mehrabi M, Rostami M. Structural and magnetic properties of CoFe2O4 ferrite nanoparticles doped by gadolinium. *Nanotechnology*. 2022;33(4):pp.13. doi:10.1088/1361-6528/ac31e8
59. Bhadra BN, Mondol MMH, Jhung SH. Metallic cobalt-anchored carbon with non-metallic heteroatom decoration: Remarkably effective oxidative desulfurization catalyst. *Sep Purif Technol*. 2024;330:125425. doi:10.1016/j.seppur.2023.125425
60. Hassanzadeh-Afruzi F. Turn over number (TON) and turn over frequency (TOF) studies for heterogeneous micro and nanocomposite catalysts. In: *Heterogeneous Micro and Nanoscale Composites for the Catalysis of Organic Reactions*. ; 2021. doi:10.1016/B978-0-12-824527-9.00004-6
61. Jangi F, Rahemi N, Allahyari S. Oxidative desulfurization using nanocomposites of heterogeneous phosphotungstic acid over natural zeolites; optimization by central-composite design. *Pet Sci Technol*. 2023;41(1):104-122. doi:10.1080/10916466.2022.2039703
62. Wang S, Patehebieke Y, Zhou Z, Zhang Z, Wang X. Catalyst-free biphasic oxidation of Thiophenes in continuous-flow. *J Flow Chem*. Published online 2020. doi:10.1007/s41981-020-00102-9
63. Wang C, Ying C, Tang Y, Yan Y, Feng X. Synergistic effect of Co(II) doping on FeS activating heterogeneous Fenton processes toward degradation of Rhodamine B. *Chemical Engineering Journal Advances*. 2020;4:100044. doi:10.1016/j.ceja.2020.100044
64. Betiha MA, Rabie AM, Ahmed HS, Abdelrahman AA, El-Shahat MF. Oxidative desulfurization using graphene and its composites for fuel containing thiophene and its derivatives: An update review. *Egyptian Journal of Petroleum*. Published online 2018. doi:10.1016/j.ejpe.2017.10.006
65. Sikarwar P, Gosu V, Subbaramaiah V. An overview of conventional and alternative technologies for the production of ultra-low-sulfur fuels. *Reviews in Chemical Engineering*. 2019;35:669-705. doi:10.1515/revce-2017-0082
66. Sikarwar P, Kumar UKA, Gosu V, Subbaramaiah V. Synergetic Effect of Cobalt-Incorporated Acid-Activated GAC for Adsorptive Desulfurization of DBT under Mild Conditions. *J Chem Eng Data*. 2018;63(8):2975-2985. doi:10.1021/acs.jced.8b00249
67. Rajakovich LJ, Zhang B, McBride MJ, Boal AK, Krebs C, Bollinger JM. Emerging structural and functional diversity in proteins with dioxygen-reactive dinuclear transition metal cofactors. In: *Comprehensive Natural Products III*. ; 2020. doi:10.1016/B978-0-12-409547-2.14864-4
68. Ouyang H, Zhang L, Jiang S, Wang W, Zhu C, Fu Z. Co Single-Atom Catalysts Boost Chemiluminescence. *Chemistry - A European Journal*.2020;26(34).doi:10.1002/chem.202002330